A More Accurate Projection in the Rate-Controlled Constrained Equilibrium Method for Dimension Reduction of Combustion Chemistry

Q. Tang*† and S.B. Pope
Sibley School of Mechanical and Aerospace Engineering
Cornell University
Ithaca, NY 14850

Abstract
An extension of the rate-controlled constrained equilibrium (RCCE) is proposed and tested. We show that RCCE contains a hidden assumption of an orthogonal projection which projects the rate equation of the chemical system onto the constrained equilibrium manifold (CEM). The extension of RCCE is obtained by making an alternative projection based on the conjecture that, near the CEM, there is a close parallel inertial manifold (CPIM). The CPIM assumption introduces the chemical kinetics directly through the local Jacobian, and hence leads to greater accuracy than RCCE.

Introduction

In the past two decades, one of the most important triumphs in combustion research is the numerical simulation of laminar flames in one or two spatial dimensions, taking account of detailed transport and chemical kinetics [1, 2]. However, for most practical reacting flows featuring three dimensional geometric complexity and turbulence, a detailed numerical simulation will remain computationally prohibitive, even on the largest supercomputers [3]. To make calculations of turbulent combustion with realistic chemistry feasible, it is necessary to reduce the computational cost of solving the complex thermo-chemical system.

The recent work of Tang and Pope [4] describes a unified dimension reduction/storage retrieval methodology which can be used to implement detailed hydrocarbon chemistry efficiently in turbulent combustion calculations. Dimension reduction is achieved through rate-controlled constrained equilibrium (RCCE) [5]; and storage/retrieval through *in situ* adaptive tabulation (ISAT) [6]. In this context, RCCE is preferred over other reduction methodologies, such as quasi-steady state assumption (QSSA) [7] and intrinsic low-dimensional manifold (ILDM) [8], because of the guaranteed existence and smoothness of the implied low-dimensional constrained equilibrium manifold (CEM). However, RCCE is solely based in thermodynamics, whereas QSSA and ILDM are appropriately based on dynamical-systems approached to the chemical kinetics. Its "efficiency" is questionable, therefore, since it is not clear that the implied reduction assumptions are near optimal.

In this study, an orthogonal projection contained in the traditional RCCE method, which projects the rate equation of the chemical system onto the constrained equilibrium manifold, is identified. A more accurate projection, which we refer to as the close parallel inertial manifold (CPIM) is then constructed. The CPIM assumption introduces the chemical kinetics directly through the local Jacobian of the chemical reacting system, and hence leads to greater accuracy then RCCE.

The remainder of the paper is organized as follows. A brief description of the rate-controlled constrained equilibrium method is provided first. In the next section we show that there is a hidden assumption in RCCE (i.e., the orthogonal projection). An alternative assumption of the CPIM and its implementation in terms of Lagrange multipliers are then proposed. The comparison between the RCCE method and its extension is made in the test calculations of hydrogen-air and methane-air autoignition. Conclusions are drawn in the final section.

Rate-Controlled Constrained Equilibrium

The rate-controlled constrained equilibrium method was introduced by Keck and Gillespie [5], it is reviewed by Keck [9], and some recent advances are described by Hamiroune et al. [10] and Yousefian [11]. In this method, it is assumed, as in thermodynamics, that fast reactions exist which relax the chemical system to the associated constrained equilibrium state on a time scale shorter than that on which the constraints are changing. In other words, a non-equilibrium system will relax to its final equilibrium state through a sequence of rate-controlled constrained equilibrium states determined by the instantaneous values of n_c constraints imposed by slow rate-limiting reactions. For a mixture (with n_s species) at a fixed pressure, p, and constant enthalpy, H, the constrained-equilibrium composition is defined to be that which maximizes the entropy $S(\mathbf{N}, p, H)$ subject to n_c linear equality constraints

* Corresponding author: qtang@mae.cornell.edu
† Current address: Reaction Engineering International, 77 West 200 South, Salt Lake City, UT 84101
Proceedings of the Third Joint Meeting of the U.S. Sections of The Combustion Institute

$$\mathbf{B}^{\mathrm{T}}\mathbf{N} = \mathbf{c}\,, \tag{1}$$

where $\mathbf{B}$ is a specified n_s x n_c constraint matrix, $\mathbf{N}$ is the vector of species mole numbers. The $n_R=n_s-n_c$ implied dimension reduction conditions can be written

$$(\mathbf{B}^{\perp})^{\mathrm{T}}\nabla S = 0\,, \tag{2}$$

where the n_R columns of $\mathbf{B}^{\perp}$ span the orthogonal complement of span($\mathbf{B}$) – the constraint subspace $\mathcal{B}$. Thus a constrained equilibrium manifold (CEM) can be defined as all compositions $\mathbf{N}$ satisfying the (constrained) maximum-entropy condition Eq.(2); and the CEM is parameterized by the constraint vector $\mathbf{c}$.

At constant temperature T and pressure p, the constrained equilibrium composition $\mathbf{N}^{\mathrm{CE}}$ can be easily computed using the method of Lagrange multipliers [12], where the following n_c+1 nonlinear equations can be solved for the Lagrange multipliers $\boldsymbol{\lambda}$ and the total moles of the mixture $\overline{N}$,

$$\begin{aligned} &\overline{N}\mathbf{B}^{\mathrm{T}}\mathbf{x} = \mathbf{c} \\ &\sum_{i=1}^{n_s} x_i = 1 \end{aligned} \tag{3}$$

with $\mathbf{x}$ being the vector of the mole fractions of species on the CEM,

$$\mathbf{x} = \exp\left(-\mathbf{g} + \mathbf{B}\boldsymbol{\lambda}\right) \tag{4}$$

and $\mathbf{g}$ the normalized molar specific Gibbs function. $\mathbf{N}^{\mathrm{CE}}$ is computed as

$$\mathbf{N}^{\mathrm{CE}} = \overline{N}\mathbf{x} \tag{5}$$

More detailed description of this method can be found in [9, 13].

Projections in RCCE

We now show that there is a hidden assumption (of an orthogonal projection) in RCCE. The constraint equation, Eq.(6), is

$$\mathbf{c} = \mathbf{B}^{\mathrm{T}}\mathbf{N}^{\mathrm{CE}} \tag{6}$$

from which the RCCE evolution equation - the rate equation of constraints, Eq.(7),

$$\dot{\mathbf{c}} = \mathbf{B}^{\mathrm{T}}\dot{\mathbf{N}}^{\mathrm{CE}} = \mathbf{B}^{\mathrm{T}}\mathbf{r} \tag{7}$$

appears to follow without assumption (since the constraint matrix $\mathbf{B}$ is independent of time), where $\mathbf{r}$ is the rate-of-change vector due to reaction. However, a geometric view of the problem exposes a hidden assumption. Figure 1 shows a sketch of the constrained equilibrium manifold (CEM) in the n_s-dimensional species space. This space is represented in the sketch by an axis span($\mathbf{B}$) for the constraint subspace $\mathcal{B}$, and an axis span($\mathbf{B}$)$^{\perp}$ for the unrepresented subspace $\mathcal{U}$. The sketch shows the rate-of-change vector $\mathbf{r}$ at the general point $\mathbf{N}$ on the CEM. An important observation is that $\mathbf{r}$ is not in the tangent space of the CEM, and so (for infinitesimal dt), $\mathbf{N}+\mathbf{r}dt$ is not on the CEM, since in general the CEM is not an inertial manifold. However, by assumption all represented compositions lie on the manifold, and hence it is necessary to project $\mathbf{r}$ onto the manifold. With $\mathbf{P}$ denoting the projection, the sketch shows that $\mathbf{Pr}$ is in the tangent space of the CEM.

To achieve dimension reduction, we wish to represent the process in the constraint subspace, which is accomplished by projecting orthogonally onto $\mathcal{B}$, yielding

$$\dot{\mathbf{c}} = \mathbf{B}^{\mathrm{T}}\mathbf{P}\dot{\mathbf{N}} = \mathbf{B}^{\mathrm{T}}\mathbf{P}\mathbf{r} \tag{8}$$

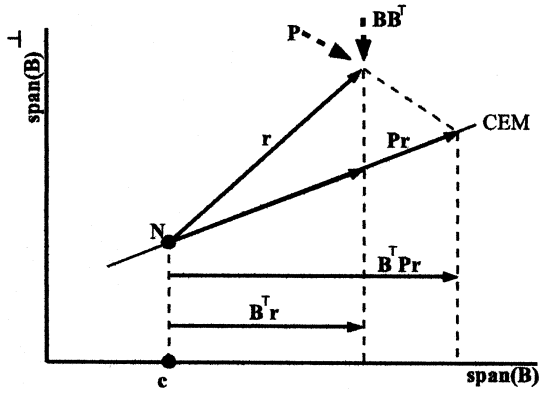

Figure 1: Sketch of the constrained equilibrium manifold (CEM) in the species space (represented by the constraint subspace $\mathcal{B}$ and the unrepresented subspace $\mathcal{U}=\mathcal{B}^{\perp}$). For simplicity the CEM is shown as being plane.

Both from the sketch and by comparing Eq. (7) and Eq. (8) it may be seen that RCCE contains the hidden assumption that $\mathbf{P}$ is a projection onto the CEM in the unrepresented subspace, and hence perpendicular to the constraint subspace. It is well appreciated (e.g., from ILDM theory) that the appropriate projection is in the fast subspace, which could be very different from the projection implied by the RCCE *method, because the fast* subspace is determined by the local Jacobian, and is generally not the fixed unrepresented subspace $\mathcal{U}$.

An Alternative Projection – CPIM

The discussion so far has revealed that it is possible to improve the accuracy of RCCE in dimension reduction

of chemical mechanism by making some alternative projections, while maintaining all represented compositions on the CEM.

We first give the definition of the local Jacobian matrix **J**(**N**), which is n_s x n_s with elements

$$J_{ij} \equiv \frac{\partial r_i}{\partial N_j} . \tag{9}$$

The eigenvalues of **J** characterize the time scales associated with the reactive system. For an infinitesimal change of the composition vector δ**N**, the rate-of-change vector can be expressed as

$$\mathbf{r}(\mathbf{N} + \delta\mathbf{N}) = \mathbf{r}(\mathbf{N}) + \mathbf{J}(\mathbf{N})\,\delta\mathbf{N} . \tag{10}$$

An alternative projection which involves the local Jacobian, and hence the chemical kinetics, can be obtained based on the hypothesis that, close to the CEM and parallel to it, there is an inertial manifold. We refer to it as the close parallel inertial manifold (CPIM).

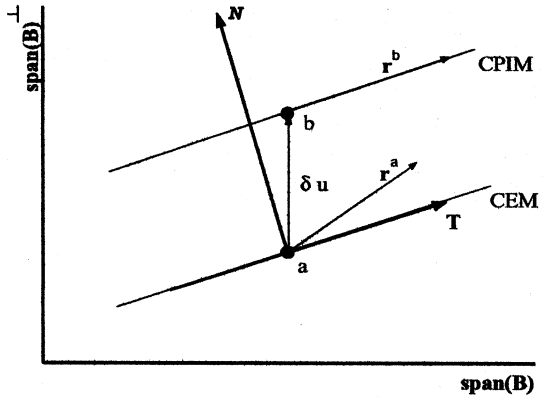

Figure 2: Sketch of the close parallel inertial manifold (CPIM) in the species space (represented by the constraint subspace $\mathcal{B}$ and the unrepresented subspace $\mathcal{U}=\mathcal{B}^{\perp}$). For simplicity the CEM is shown as being plane.

Figure 2 shows the sketch of the CPIM together with the CEM in the species space (represented by the constraint subspace $\mathcal{B}$ and the unrepresented subspace $\mathcal{U}$). In the sketch the point (a) is on the CEM with the composition being $\mathbf{N}^a$, and the rate-of-change vector $\mathbf{r}^a$. $\mathcal{T}$=span(**T**) and $\mathcal{N}$=span(**Ω**) represent the tangent space of the CEM and its normal subspace, respectively, where **T** is n_s x n_c and **Ω** is n_s x n_R, and can be derived analytically from the nonlinear equation system Eq. (3)-Eq. (5) (see [13] for detail). The point (b) lies on the CPIM with the composition being $\mathbf{N}^b$, which satisfies the condition

$$\mathbf{B}^T\mathbf{N}^b = \mathbf{B}^T\mathbf{N}^a . \tag{11}$$

Hence the difference between $\mathbf{N}^b$ and $\mathbf{N}^a$ lies entirely in the subspace $\mathcal{U}$, and can be expressed as

$$\delta\mathbf{N} = \mathbf{N}^b - \mathbf{N}^a = \mathbf{U}\,\delta\mathbf{u} , \tag{12}$$

where δ**u** is an n_R-vector, and the columns of **U** span the subspace $\mathcal{U}$. The rate-of-change vector at point (b) is denoted by $\mathbf{r}^b$, and by the assumption that the CPIM is an inertial manifold, its components in the normal subspace $\mathcal{N}$ are zero:

$$\mathbf{\Omega}^T\mathbf{r}^b = 0 . \tag{13}$$

Using the linear approximation we have

$$\mathbf{r}^b = \mathbf{r}(\mathbf{N}^b) = \mathbf{r}^a + \mathbf{J}\mathbf{U}\,\delta\mathbf{u} . \tag{14}$$

Thus the condition Eq.(13) yields

$$\mathbf{\Omega}^T\mathbf{r}^b = 0 = \mathbf{\Omega}^T\left(\mathbf{r}^a + \mathbf{J}\mathbf{U}\,\delta\mathbf{u}\right), \tag{15}$$

and hence

$$\delta\mathbf{u} = -\mathbf{K}^{-1}\mathbf{\Omega}^T\mathbf{r}^a , \tag{16}$$

where the n_R x n_R matrix **K** is

$$\mathbf{K} = \mathbf{\Omega}^T\mathbf{J}\mathbf{U} . \tag{17}$$

Substituting Eq. (16) into Eq. (14), we obtain the rate-of-change vector $\mathbf{r}^b$ on CPIM in terms of $\mathbf{r}^a$,

$$\begin{aligned} \mathbf{r}^b &= \mathbf{r}^a + \mathbf{J}\mathbf{U}\delta\mathbf{u} \\ &= \left(\mathbf{I} - \mathbf{J}\mathbf{U}\mathbf{K}^{-1}\mathbf{\Omega}^T\right)\mathbf{r}^a \\ &= \mathbf{T}\mathbf{T}^T\left(\mathbf{I} - \mathbf{J}\mathbf{U}\mathbf{K}^{-1}\mathbf{\Omega}^T\right)\mathbf{r}^a \end{aligned} \tag{18}$$

The product $\mathbf{T}\mathbf{T}^T$ defines an orthogonal projection onto $\mathcal{T}$. Since $\mathbf{r}^b$ lies in the tangent subspace, $\mathbf{T}\mathbf{T}^T\mathbf{r}^b = \mathbf{r}^b$, and the last step in Eq. (18) follows. The difference between $\mathbf{r}^b$ and $\mathbf{r}^a$ can be viewed in two parts: first, the removal of the normal component, yielding $\mathbf{T}\mathbf{T}^T\mathbf{r}^a$; and second, a modification to the tangential component, i.e., the addition of $-\mathbf{T}\mathbf{T}^T\mathbf{J}\mathbf{U}\mathbf{K}^{-1}\mathbf{\Omega}^T\mathbf{r}^a$. Note that the first modification amounts to the perpendicular projection of $\mathbf{r}^a$ onto $\mathcal{T}$, and is well-conditioned independent of **K**.

Using the sketch shown in Figure 2, the projection implied by the CPIM assumption is

$$\mathbf{P} = \mathbf{I} - \mathbf{J}\mathbf{U}\mathbf{K}^{-1}\mathbf{\Omega}^T , \tag{19}$$

and the rate equation of constraints using CPIM becomes

$$\dot{\mathbf{c}} = \mathbf{B}^T\mathbf{P}\mathbf{r} , \tag{20}$$

where $\mathbf{r}$ is evaluated on the CEM.

Apparently, the success of CPIM relies on two key assumptions. First is that the distance between the CEM point and its counterpart on the CPIM is small enough so that the linear approximation Eq. (14) is valid; and second, the principal angles between the tangent subspace of the CEM and the tangent subspace of the attracting inertial manifold $\mathcal{M}$ are small, given the same level of dimension reduction. It can be expected that if the CEM is a good approximation to $\mathcal{M}$ (i.e., close to $\mathcal{M}$), CPIM leads to greater accuracy than CEM.

Rate Equation of Lagrange Multipliers

We now consider the simplest case of a reactive ideal gas mixture, although the methodology developed is generally applicable to other complex situations. The system is spatially homogeneous, adiabatic, and isobaric. The thermo-dynamical state of the mixture is completely determined by $n_s + 2$ variables, namely the species mole number $\mathbf{N}$, the enthalpy H, and the pressure p. The equation system that describes the time-dependent development of these properties can be written as

$$\dot{H} = 0; \quad \dot{p} = 0, \tag{21}$$

$$\dot{\mathbf{N}} = \mathbf{r}. \tag{22}$$

In RCCE, only the rate equations for the n_c constraints $\mathbf{c}$ are needed to determine the state of the system, given H and p. The rate equation for $\mathbf{c}$ Eq. (7) is restated here

$$\dot{\mathbf{c}} = \mathbf{B}^T\dot{\mathbf{N}} = \mathbf{B}^T\mathbf{r}. \tag{23}$$

Note that the rate-of-change vector $\mathbf{r}$ is now a function of the constrained equilibrium composition $\mathbf{N}^{CE}$ at given H and p.

Given the initial conditions, equations (21) and (23) can be integrated together in a stepwise fashion. Since $\mathbf{r}$ must be evaluated on the CEM, at each step the constrained equilibrium composition must be computed via solving the $n_c + 1$ nonlinear equation system (3), (4) and (5). For this reason the calculations for small systems, in which the number of species is not very much larger than the number of constraints, may take more CPU time than that required to integrate the full set of rate equations.

In fact, the RCCE problem can be solved in a totally different way without pursuing the constrained equilibrium composition via solving a complex nonlinear system many times. The alternative approach is to integrate the rate equations for the Lagrange multipliers. As shown in Eq. (3) and (4), for each constraint there is a corresponding Lagrange multiplier, and the constrained equilibrium composition is explicitly determined by $\boldsymbol{\lambda}$ through Eq. (5). This approach was first suggested by Keck [9], and reviewed by Hamiroune et al. [10] later.

Starting from the nonlinear equation system – Eq. (3) - (5), which determines the CEM, the rate equation of Lagrange multiplier can be derived, and can be written in matrix form [13]

$$\begin{bmatrix} \mathbf{I} & \mathbf{E}_T & \mathbf{0} \\ \mathbf{F}^T & G_T & G_c \\ \mathbf{0} & 0 & 1 \end{bmatrix} \begin{bmatrix} \dot{\boldsymbol{\lambda}} \\ \dot{T} \\ |\dot{\mathbf{c}}| \end{bmatrix} = \begin{bmatrix} \boldsymbol{\xi} \\ 0 \\ R_c \end{bmatrix}, \tag{24}$$

where $\mathbf{I}$ is an n_c x n_c identity matrix; $\mathbf{E}_T$ and $\mathbf{F}^T$ are n_c x 1 and 1 x n_c vectors, respectively; G_T and G_c are scalars. The detailed procedure of the derivation of Eq. (24) , and the definitions of the variables in the equation can be found in [13]. In particular, the n_c x 1 vector $\boldsymbol{\xi}$ on the right-hand side is a function of $\boldsymbol{\theta}$ with

$$\boldsymbol{\theta} \equiv \frac{1}{N}\left(\mathbf{I} - \frac{\mathbf{c}\mathbf{c}^T}{\mathbf{c}^T\mathbf{c}}\right)\mathbf{B}^T\mathbf{r}, \tag{25}$$

and the scalar R_c is defined as

$$R_c \equiv \frac{\mathbf{c}^T\mathbf{B}^T\mathbf{r}}{|\mathbf{c}|}. \tag{26}$$

For CPIM, the equations describe the time evolving of $\boldsymbol{\lambda}$, T, and $|\mathbf{c}|$ are of the same forms as those in Eq. (24). The differences are

$$\boldsymbol{\theta} \equiv \frac{1}{N}\left(\mathbf{I} - \frac{\mathbf{c}\mathbf{c}^T}{\mathbf{c}^T\mathbf{c}}\right)\mathbf{B}^T\mathbf{P}\mathbf{r}, \tag{27}$$

and

$$R_c \equiv \frac{\mathbf{c}^T\mathbf{B}^T\mathbf{P}\mathbf{r}}{|\mathbf{c}|}, \tag{28}$$

where $\mathbf{P}$ is defined in Eq. (19).

The two approaches to solve the RCCE problem, namely, solving the rate equation of constraints Eq. (23), or solving the rate equation of Lagrange multipliers Eq. (24), are fully consistent, provided that the integrating time step in the first approach tends to zero.

Test Results and Discussion

Two combustion systems are chosen, namely the H_2/Air system ($n_s = 9$) and the CH_4/Air (GRI1.2, $n_s = 31$) system, For more information about the two detailed mechanisms, see [14] and [15].

The test calculations are made in the idealized Plug-Flow-Reactor (PFR), where a premixed mixture of fuel-air evolves from its initial state eventually to the complete equilibrium state. We refer to this test as the auto-ignition

test case. The rate equation of Lagrange multipliers is integrated in all RCCE and CPIM calculations. The results are then compared with the exact solutions using the detailed mechanisms and the full set of rate equation of species. All calculations are adiabatic and isobaric.

For the H_2/Air system, in addition to the time independent constraints imposed by the conservation of elements, three time dependent linear constraints are used in the calculation. Among them are: total number of moles, denoted by TM, which is imposed by slow dissociation/recombination reactions; "active valence" (AV = H + OH + 2O), which is related to the total number of radicals, and is imposed by the slow branching reactions; and "free oxygen" (FO = O + OH + H_2O), which is defined as any oxygen that is not bonded to another oxygen, and is imposed by the reactions where the O-O bond is broken.

Figure 3 shows the calculated temperatures against time using two time dependent constraints ($n_c = 5$). Φ is

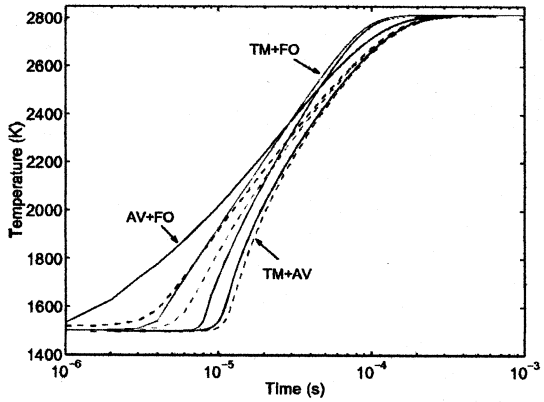

Figure 3: Temperature as a function of time using two time-dependent constraints (T_0 = 1500 K, p = 1 atm, and Φ = 1). Black solid line: exact solution; Other solid lines: RCCE; Dashed lines: CPIM; Red: TM+AV; Blue: AV+FO; Green: TM+FO.

the equivalence ratio. The comparisons of the results between the CPIM and the RCCE calculations are very encouraging. In each of the three combinations, the CPIM result shows greater accuracy (dashed line) than that of RCCE (solid line in the same color as that of CPIM result) without exception, especially for the case using TM + AV (red dashed line), the result is in excellent agreement with the exact solution throughout the calculation. The comparisons among the three CPIM calculations shows that, in the high temperature range (T > 2400 K), the temperature-time curves are all very close to the accurate result. However, in predicting the ignition delay, the errors in the cases using TM + FO and AV + FO are still high with the latter one giving the worst result. Nevertheless, the results plotted in Figure 3 shows that the CPIM calculations are less dependent on the choices of the constraint subspace than the RCCE calculations.

The effects of the number of constraints are shown in Figure 4. Starting from the calculation using TM, we add the other constraints one at a time in the order AV then FO. For RCCE, using TM only is not able to predict the

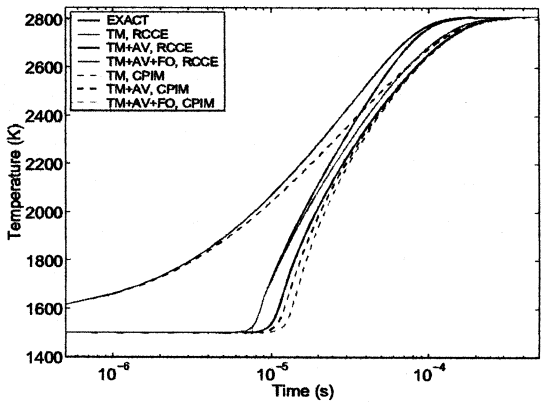

Figure 4: Effects of the number of constraints on RCCE/CPIM calculations (T_0 = 1500 K, p = 1 atm, and Φ = 1). Black solid line: exact solution; Other solid lines: RCCE; Dashed lines: CPIM.

temperature-time curve correctly. The addition of AV improves the result dramatically in the lower temperature range, which results in a much better prediction of the ignition delay time. The benefit from FO is mainly seen in the higher temperature range (T>1800 K). For CPIM, the improvement is observed in the higher temperature range (T > 2000 K) for the case using TM only. The case using TM and AV is still the best one, while the case using all three variable constraints predicts ignition delay time slightly longer, which implies that the addition of FO may have some negative impacts on the CPIM assumption.

Table 1: Variable constraints for the CH_4/Air system

Case 1 (n_c=16)	TM, AV, CO_2, H_2O, CH_4, O_2, CO, CH_3, H_2, C_2H_2, C_2H_4, C_2H_6
Case 2 (n_c=16)	TM, AV, CO_2, H_2O, CH_4, O_2, CO, CH_3, H_2, C_2H_2, HO_2, H_2O_2
Case 3 (n_c=18)	TM, AV, CO_2, H_2O, CH_4, O_2, CO, CH_3, H_2, C_2H_2, C_2H_4, C_2H_6, HO_2, H_2O_2
Case 4 (n_c=20)	TM, CO_2, H_2O, CH_4, O_2, CO, CH_3, H_2, C_2H_2, C_2H_4, C_2H_6, HO_2, H_2O_2, H, OH, O

For the CH_4/Air system, four time independent constraints on elements are used in all calculations. The selection of time dependent constraints is mainly based on experience and a trial and error process. In addition to constraints TM and AV defined in the H_2/Air calculation, constraints are imposed on individual species number of

mole. Four cases with different sets of constraints are summarized in Table 1.

Figure 5 shows the evolutions of temperature and mole fractions of major species calculated in all four cases. It is noticed that for all cases, the CPIM results predict the ignition delay time accurately, and the shapes of the time evolutions of temperature and major species are reproduced nearly perfectly. The differences among the four cases for these quantities are negligible. In contrast, the RCCE calculations in these cases are not able to compete with CPIM in terms of accuracy. This suggests that at the higher temperature range (i.e., T>1500 K), the close parallel inertial manifold is a good approximation to the slow attracting manifold, and the CPIM is not very sensitive to the choice of constraint subspace, whereas for RCCE, the correlation is strong.

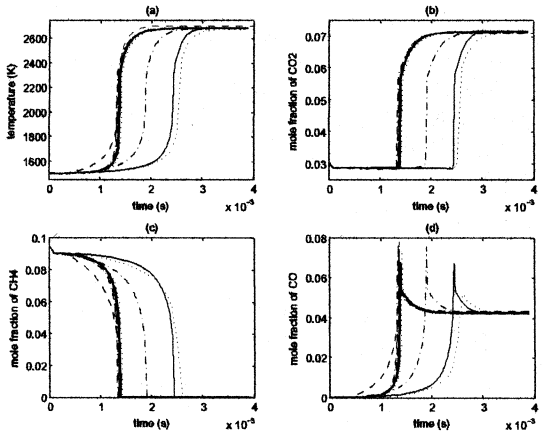

Figure 5: Comparisons of major species mole fractions against time calculated using RCCE and CPIM (T_0 = 1500 K, p = 1 atm, and Φ =1). Black: exact solution; Red: CPIM; Blue: RCCE; Solid line: Case 1; Dashed line: Case 2; Dash-dot line: Case 3; Dotted line: Case 4

The main differences among these cases are highlighted in Figure 6. It may be seen that the mole fractions of HO_2 and H_2O_2 are not well predicted in Case 1, while they are accurately predicted in the other three cases.

Conclusions

The CPIM method shows great promise in improving the dimension reduction accuracy. In the test calculations, with an initial temperature T_0 = 1500 K, the CPIM results are in excellent agreement with the exact solution using the detailed mechanism, and are much better than the corresponding RCCE calculations, while the dimension reductions are from 9 to 5, and from 31 to 16, for the two reaction systems, respectively.

The CPIM method shows less dependence upon the choice of constraint subspace. In the calculations for CH_4/Air system (T_0 = 1500 K), the CPIM calculations with four different sets of constraints achieve the same level of accuracy. On the contrary, the performance of RCCE is very sensitive to the choice of constraints.

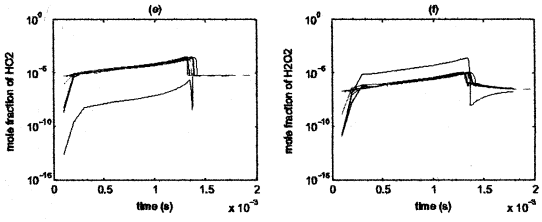

Figure 6: Comparisons of minor species mole fractions against time calculated using CPIM (T_0 = 1500 K, p = 1 atm, and Φ = 1). Black: exact solution; Red: Case 1; Blue: Case 2; Green: Case 3; Magenta: Case4.)

Acknowledgement

This work is supported by Air Force Office of Scientific Research grant F-49620-00-1-0171.

References

[1] Dixon-Lewis, G., David, T., Gaskell, P.H., Fukutani, S., Jinno, H., Miller, J.A., Kee, R.J., Smooke, M.D., Peters, N., Effelsberg, E., Warnatz, J., and Behrentl. F., *Proc. Combust. Inst.*, 20:1893 (1984).

[2] Smooke, M.D., Crump, J., Seshadri, k., and Giovangigli, V., *Proc. Combust. Inst.*,23:463-470, (1990).

[3] Pope. S.B., *Proc. Combust. Inst.*, 23: 591-612, (1990).

[4] Tang, Q., and Pope, S.B., *Proc. Combust. Inst.*, to appear, (2002).

[5] Keck, J.C., and Gillespie, D. *Combust. Flame*, 17:237-241, (1971).

[6] Pope. S.B., *Combust. Theo. Modeling*, 1:41-63, (1997).

[7] Bodenstein, M., and Lind. S.C., *Z. Phys. Chem.*, 57:168, (1906).

[8] Maas, U. and Pope. S.B., *Combust. Flame*, 88:239-264, (1992).

[9] Keck, J.C. *Prog. Energy Combust. Sci.*, 16:125-154, (1990).

[10]Hamiroune, D., Bishnu, P., Metghalchi, M., and Keck, J.C., *Combust. Theo. Modelling*, 2:81-94 (1998).

[11] Yousefian, V., *Combust. Flame*, 115:66-80, (1998).

[12] Reynolds, W.C., *Report*, Mechanical Engineering Department, Stanford University, (1986).

[13] Tang, Q., *Ph.D thesis*, Cornell University, (2003).

[14] Maas, U., and Warnatz, J., *Proc. Combust. Inst.*, 22:1695, (1988).

[15] Frenklach, M., Wang, H., Goldenberg, M., Smith, G.P., Golden, D.M., Bowman, C.T., Hanson, R.K., Gardiner, W.C., and Lissianski, V., *Gas Research Institute Topical Report*, Report No.GRI-95/0058, (1995).